Theory of acoustic attenuation, dispersion, and pulse propagation in unconsolidated granular materials including marine sediments

Michael J. Buckingham[a)]
Marine Physical Laboratory, Scripps Institution of Oceanography, University of California, San Diego, 9500 Gilman Drive, La Jolla, California 92093-0213

(Received 7 August 1996; revised 25 November 1996; accepted 31 July 1997)

A unified theory of sound propagation in saturated marine sediments is developed on the basis of a linear wave equation, which includes a new dissipation term representing internal losses arising from interparticle contacts. This loss mechanism, which shows a ''memory'' or hysteresis, is proposed as being responsible for the acoustic properties of sediments. To accommodate the memory, the loss term in the wave equation is formulated as a temporal convolution between the particle velocity and a material response function, $h(t)$, which varies as t^{-n}, where $0<n<1$. The compressional wave that emerges from the analysis shows: (1) an attenuation that scales almost exactly as the first power of frequency (corresponding to a constant Q) over an unlimited number of decades; and (2) weak logarithmic dispersion. As well as being characteristic of the wave properties of actual marine sediments, the predicted attenuation and dispersion are consistent with the Kronig–Kramers relationships. The theory also leads to pulse propagation that is strictly causal, which, although a necessary requirement, is an issue that has been widely debated in the literature in the context of an attenuation that is proportional to frequency. Finally, the wave properties (phase speed and attenuation) are related to the mechanical properties (grain size, density, and porosity) of a sediment by combining the Hertz theory of particles in contact with a new, rough-surface, random-packing model of mineral grains in unconsolidated granular media. The resultant relationships between the acoustical and mechanical properties (e.g., sound speed and porosity) of marine sediments are shown to follow the trends of published experimental data sets very closely.
 [S0001-4966(97)04411-1]

PACS numbers: 43.30.Ma [JHM]

LIST OF SYMBOLS

c_p	compressional wave speed (m/s)
c_0	compressional wave speed in absence of intergranular friction (m/s)
α_p	compressional attenuation coefficient (nepers/m)
β_p	compressional loss tangent
Q	quality factor
χ_f	compressional dissipation coefficient
μ_c	compressional frictional rigidity modulus
ω	angular frequency
k_0	wave number in absence of intergranular friction
t	time
p	pressure fluctuation
v	particle velocity
ρ	density fluctuation
$\psi(t)$	velocity potential
$\Psi(j\omega)$	Fourier transform of $\psi(t)$
$h(t)$	material memory function
$H(j\omega)$	Fourier transform of $h(t)$
n	material memory exponent $(0<n<1)$
u_g	mean grain diameter, microns
N	porosity $(0<N<1)$
ρ_0	bulk density of sediment (kg/m^3)
κ	bulk modulus of sediment (Pa)
γ	volume ratio of smaller to larger grains in a bimodal sediment
$\rho_w=1024$ kg/m^3	density of pore water
$\rho_g=2700$ kg/m^3	density of mineral grains
$\kappa_w=2.25\times10^9$ Pa	bulk modulus of pore water
$\kappa_g=1.47\times10^{10}$ Pa	bulk modulus of mineral grains
$\Delta=3$ μm	rms particle roughness
$P=0.63$	packing factor of randomly packed smooth spheres
$u_0=1000$ μm	reference grain diameter
$\mu_0=2\times10^9$ Pa	compressional frictional rigidity constant

INTRODUCTION

A substantial body of data supports the view that compressional-wave attenuation in many porous, granular materials varies more or less accurately as the first power of frequency, f^1, over an extended frequency range, from 1 Hz up to 1 MHz. The evidence for this observation has been extensively discussed in a nicely argued review of the sub-

[a)]Also affiliated to: Institute of Sound and Vibration Research The University, Southampton SO17 1BJ, England.

ject by Kibblewhite,[1] which includes a comprehensive bibliography covering much of the relevant literature.

A striking conclusion from Kibblewhite's[1] careful examination of the available data is that, in at least one class of granular materials, i.e., dry sandstones, the attenuation scales accurately with the first power of frequency from seismic to high ultrasonic frequencies, a frequency range of some six decades. The fact that in dry, consolidated, porous media the attenuation varies as f^1 over so many decades suggests that this type of attenuation may be attributed to a single loss mechanism, which can be identified from the geophysics literature as an unspecified form of internal dissipation[2–5] arising at grain-to-grain contacts.

The question of whether attenuation in saturated, unconsolidated marine sediments is accurately proportional to the first power of frequency is still under debate. Hamilton[6,7] has long argued, on the basis of extensive experimental evidence, that attenuation in marine sediments does indeed exhibit an f^1 dependence, a point of view which is shared by other investigators.[8] On the other hand, Kibblewhite[1] concludes from the data of Hamilton[6,7] and others that attenuation in fluid-saturated sediments does not accurately follow the f^1 law. In these materials, he argues, there appear to be two mechanisms responsible for the attenuation, one being ''internal friction,'' which somehow gives rise to a linear scaling with frequency, as in dry materials, and a second due to the viscosity of the pore fluid.[5] The effects of viscosity, if any, are said to manifest themselves globally through the relative motion of the pore fluid and the sediment frame (if this has any meaning in the context of an unconsolidated medium), and also locally through fluid motion in the neighbourhood of interparticle contacts. According to Kibblewhite's argument, these additional viscous loss components are responsible for any deviation from the f^1 law in saturated materials.

It is evident from Kibblewhite's discussion[1] that internal dissipation, which is frequently stated (without proof) as giving rise to the proportionality between attenuation and frequency, is a fundamentally important physical phenomenon exhibited by granular materials,[9] irrespective of whether they are dry or wet. In the case of the latter, it seems that viscous losses could also be present, but to a degree that is still uncertain. The term *characteristic attenuation* is introduced here to identify the component of attenuation that scales accurately as f^1, corresponding to a constant quality factor,[10] or Q. (A possible alternative term is *intrinsic attenuation*, but this is already in use[1] to describe all internal loss mechanisms, such as internal friction and pore-fluid viscosity, but excluding losses due to scattering and also energy conversion losses arising from coupling between compressional and shear waves.)

A number of theories of attenuation in granular materials have been explored over the years. An early mechanism, discussed by Morse,[11] is bulk viscosity, corresponding to a frictional stress that is proportional to the particle velocity. However, viscous dissipation yields an attenuation that scales as the square of frequency[12] at low frequencies and as the square root of frequency[13] beyond some critical frequency, and hence cannot account for the characteristic attenuation. Porosity is another candidate mechanism, but it is well-known that a simple porous solid with a rigid frame, satisfying Darcy's law,[14] gives rise to an attenuation that is constant at high frequencies and scales as the square root of frequency below a critical frequency.[13,15] Again, such behavior does not match that of the characteristic attenuation.

Certain theoretical implications of a linear scaling between attenuation and frequency have been discussed by Horton[16] on the basis of the Kronig–Kramers dispersion relationships. He initially concluded that there is no dispersion in a material showing the characteristic attenuation, which is consistent with the frequency-independent sound speed observed in several field measurements.[17,18] However, in a later paper, Horton,[19] acknowledging an algebraic error in his previous analysis, pointed out that when the attenuation scales with frequency the phase speed actually shows a very slight logarithmic dispersion, in agreement with the theoretical treatment of O'Donnell *et al.*[20]

Laboratory measurements of logarithmic dispersion in saturated medium sand have been reported by Wingham,[21] at a level that agrees with O'Donnell *et al.*'s theoretical expression. However, the dispersion is so weak that a sensitive differential technique was required to detect it, which may account for the fact that it was not observed in the field measurements of McDonal[17] and Hamilton.[18] White[13] has collated a number of hypothetical attenuation-dispersion pairs that have been proposed by various authors in efforts to model the characteristic attenuation in granular materials.

For a number of years, Hamilton[22,23] has taken an empirical approach to modeling the geoacoustic properties of marine sediments. From a practical point of view, he has had great success with his models, although he does not consider the specific mechanism responsible for the attenuation. However, he does allow for the possibility of both dispersion and an attenuation that deviates from an f^1 power law.

An entirely different modeling approach is found in the classical works of Biot on the mechanics of porous, deformable media.[24–26] In his original theory, Biot assumed Poiseuille flow in a saturated porous medium with a linear elastic frame. From this model, the functional dependence of the attenuation on frequency is the same at low frequencies as that due to viscosity, scaling with the second power of frequency, f^2; and at higher frequencies it varies as f^0 (a constant). After modifying the theory to include the effects of viscosity in the vicinity of intergranular contacts, the frequency dependence of the attenuation takes the same functional form as in the case of a viscous fluid: At low frequencies the attenuation scales with f^2 and at higher frequencies it is proportional to $f^{1/2}$. Thus the Biot theory, even in its modified form, does not account for the characteristic attenuation in granular materials.

Biot's theoretical developments have been extended by Stoll[27] in a long-standing effort to model the geoacoustic behavior of marine sediments. The Biot–Stoll theory is a ''pseudo-harmonic'' analysis in which the shear and bulk moduli of an assumed skeletal frame are treated as complex quantities and assigned a frequency dependence determined from a match to data. This hybrid approach, a combination of analysis and empiricism, has had considerable success in

providing an accurate description of the geoacoustic behavior of many materials of interest to the geophysics community. However, the theory does not easily account for the characteristic attenuation exhibited by granular materials over an extended frequency range. Moreover, issues of causality and pulse propagation in porous materials, which have to be handled in the time domain, are not readily addressed within the pseudo-harmonic framework of the Biot–Stoll theory.

Although some form of internal friction has been identified experimentally as being responsible for the characteristic attenuation exhibited by granular materials,[2–5] the actual mechanism has not yielded readily to theoretical analysis. Various types of internal loss have been investigated with limited success, including a nonlinear mechanism associated with the motion of dislocations,[28] and frictional dissipation arising from the sliding of crack surfaces in contact with each other.[29] A symbolic manipulation approach to the problem of the characteristic attenuation has been developed by Verweij,[30] based on theoretical techniques developed by himself[31] and de Hoop.[32,33]

I. A NEW THEORY OF SEDIMENTS ACOUSTICS

In this article, an internally consistent, unified theory of acoustic propagation in a saturated, unconsolidated, marine sediment is developed. It is taken as axiomatic that an unconsolidated sediment is a two-phase medium, consisting of mineral particles and seawater, but possessing no rigid frame; that is to say, the elastic rigidity modulus of the medium is identically zero. Thus the material is treated as a bulk fluid in which sound propagation is governed by internal losses arising at grain-to-grain contacts. Throughout the discussion, the word ''friction'' is used exclusively and specifically to mean a new type of intergranular dissipation, which has fundamentally different properties from more familiar loss mechanisms such as viscosity or Coulomb friction.

The analysis is based on a linear wave equation in which intergranular dissipation is represented by a loss term that takes account of the hysteresis, or memory, of granular media. The effect of the memory on wave propagation is accommodated by setting the frictional stress equal to a temporal convolution between the particle velocity and a material memory function, $h(t)$. This formulation is identically that for a viscous fluid when $h(t)$ is set equal to a Dirac delta function, corresponding to the special case of a medium with no memory. A marine sediment, however, does possess a memory, the appropriate memory function being of the form $h(t) \propto t^{-n}$, where $0<n<1$. The properties of such a medium are quite different from those of say a viscous fluid.

Several interesting results emerge from the theory, including an attenuation coefficient that is almost exactly proportional to frequency over an unlimited number of decades. The model also predicts weak logarithmic dispersion which has exactly the form required by the Kronig–Kramers relationships, as well as faithfully matching that observed experimentally by Wingham.[21] An important prediction of the theory is that, with increasing frictional dissipation, the material becomes stiffer and consequently the compressional wave speed increases. In the time domain, an expression is derived for the Green's function, representing transient propagation, which is shown to be strictly causal (as of course it must be). As the intergranular friction is allowed to go to zero, the Green's function reduces in a natural way to the familiar retarded potential solution for the pulse shape in a lossless medium.

Viscosity of the pore fluid has often been suggested as being a significant loss mechanism in sediments.[27] The effects of pore fluid viscosity are examined briefly by including a conventional viscous dissipation term in the new wave equation in addition to the intergranular friction term. A solution for the attenuation coefficient is obtained which deviates at higher frequencies from the f^1 law due to intergranular friction alone; and the viscosity also introduces a greatly enhanced dispersion. Such behavior is not consistent with Wingham's[21] measurements of attenuation and dispersion in saturated sand, nor with the absence of dispersion in marine sediments reported by Hamilton.[18] This lack of experimental support provides strong evidence that, compared with intergranular friction, pore-fluid viscosity is insignificant in saturated marine sediments.

It has been confirmed experimentally[18] that the compressional wave speed in an unconsolidated sediment correlates well with the mechanical parameters (particle size, density, and porosity) of the medium, and that the porosity and density themselves are each correlated with the particle size. To establish theoretical relationships between porosity, density, and particle size, a new rough-particle, random-packing model of mineral particles is introduced. From this model of mechanical structure of the sediment, the porosity and the density are expressed as algebraic functions of the particle size.

To provide the link between the acoustic and mechanical properties of a sediment, the intergranular friction is related to the particle size by a fractional power law, as suggested by the Hertz theory of elastic spheres in contact. The final result is a set of equations which give all the acoustic and mechanical properties of sediments as simple algebraic functions of the particle size. These theoretical expressions, relating sound speed, attenuation, porosity, and density to the particle size, are valid for surficial sediments. It turns out that the theoretical relationships predicted by the combined geoacoustic models show compelling agreement with extensive, published data sets representing not only silts and all grades of sand but also the very fine-grained clays.

Sands and silts conform to the geometry of the rough-sphere model, in that the grains resemble distorted spheres. Clay particles, however, are not spherical but show a platelet structure with a high aspect ratio, which raises the question as to why they should be so well described by the rough-sphere theory? It is argued that a mineral platelet in clay may be thought of as a special (extreme) case of a rough sphere in which the magnitude of the roughness is comparable to or greater than the size of the sphere itself. In this picture, a platelet is essentially all roughness on a relatively small spherical body. Although this may be an unusual geometrical description of a clay particle, it appears to be accurate as far as packing arguments are concerned, and it brings the clays

within the unified geoacoustic theory of sediments developed here.

II. A WAVE EQUATION WITH INTER-GRANULAR FRICTION

To address the question of wave propagation in granular materials, the medium is treated as fluidlike, macroscopically homogeneous, isotropic, time invariant, and infinite. A source is assumed to excite compressional plane waves in the material and, since there are no boundaries, there is no coupling into shear waves. The propagation of the compressional waves is governed by a wave equation in which intergranular friction is represented by a very specific dissipation term, whose formulation is crucial to the argument.

Since a form of internal friction is the loss mechanism, the dissipation term must originate in the equation of motion,[34] which, for one-dimensional propagation in the x direction, is postulated to be

$$\rho_0 \frac{\partial v}{\partial t} + \frac{\partial p}{\partial x} - \left(\frac{4}{3}\,\eta_f + \lambda_f \right) \frac{\partial^2 [h(t) \otimes v(t)]}{\partial x^2} = 0, \tag{1}$$

where v is particle velocity in the x direction, p is the pressure fluctuation, t is time, ρ_0 is the bulk density, and the symbol $\otimes$ denotes a temporal convolution operation. The dissipation coefficients η_f and λ_f have been introduced by analogy with the shear and bulk viscosities of a conventional fluid, although in this case the subscript f identifies these coefficients as being associated with intergranular friction rather than viscosity.

The proposed dissipation term in Eq. (1) possesses something of the character of viscosity, in that the differential operator in the loss term is $\partial^2/\partial x^2$, but the operand, instead of being particle velocity, is the convolution of particle velocity with an impulse response function of the material, $h(t)$. Clearly, when $h(t)$ is a Dirac delta function the convolution reduces to the particle velocity, in which case the equation of motion is identically that for a viscous fluid[12] or a Voigt solid.[13] The more general form in Eq. (1) allows for the possibility that the medium ''remembers'' previous states, with a memory that is characterized by $h(t)$. A generalized description of linear internal losses in terms of convolution operations is fairly well-established in the geophysics literature.[35]

The remaining expressions necessary to derive the wave equation are standard in that they do not involve dissipation terms. Conservation of mass requires that

$$\rho_0 \frac{\partial v}{\partial x} + \frac{\partial \rho}{\partial t} = 0, \tag{2}$$

and the equation of state is

$$p = c_0^2 \rho, \tag{3a}$$

where

$$c_0 = \sqrt{\frac{\kappa}{\rho_0}}. \tag{3b}$$

In these equations, ρ is the density fluctuation and κ is the bulk modulus of the medium. According to Eq. (3b), c_0 may be interpreted as the sound speed in the medium in the absence of grain-to-grain losses. As it turns out, c_0 is an important parameter in the theory of intergranular friction; it will be expressed later in terms of the bulk properties of the two materials, i.e., the mineral grains and seawater, constituting the sediment. We shall also see that one effect of the friction is to introduce some stiffness into the medium, which raises the actual wave speed above c_0, to a degree that depends on the level of the dissipation.

On introducing a velocity potential, ψ, defined by

$$v = -\frac{\partial \psi}{\partial x}, \tag{4}$$

and combining the above equations, the following wave equation is obtained:

$$\frac{\partial^2 \psi}{\partial x^2} - \frac{1}{c_0^2} \frac{\partial^2 \psi}{\partial t^2} + \frac{(\frac{4}{3}\eta_f + \lambda_f)}{\rho_0 c_0^2} \frac{\partial^3}{\partial t\, \partial x^2} \{h(t) \otimes \psi(t)\} = -S\,\delta(t)\,\delta(x). \tag{5}$$

A driving term representing a planar, impulsive source has been included on the right, in which S is the source strength (with units of length) and $\delta(\cdots)$ is the Dirac delta function. Equation (5) is the cornerstone of the following analysis of wave propagation in a granular medium. The memory function $h(t)$ in Eq. (5) still remains to be specified, to which end the following argument is developed.

It is proposed that, although assumed to possess no skeletal frame, implying zero elastic rigidity, an unconsolidated sediment exhibits behavior resembling that of a visco-elastic solid as a result of the intergranular friction: Loads and deformations are linearly related but the deformation depends on the history of the loading process. In such a material, the response to an instantaneous stress is an instantaneous strain followed by a strain which increases with time. Such behavior in a viscoelastic material is known as ''creep.'' The converse is ''relaxation,'' in which an instantaneous strain gives rise to an instantaneous stress followed by a decrease in stress level with increasing time. Thus creep and relaxation are two sides of the same coin, and in a saturated sediment these phenomena originate in the dissipation occurring at grain-to-grain contacts.

In formulating the material response function, we use as a guide the process of relaxation. A typical relaxation function[35,36] is of the form $(1/t)$ raised to some small power, and accordingly we set

$$h(t) = u(t)\, \frac{t_0^{n-1}}{t^n}, \quad 0 < n < 1, \tag{6}$$

where $u(t)$, the unit step function, ensures that the response of the medium is causal. The scaling constant t_0 in Eq. (6), with units of time, is included explicitly to ensure that $h(t)$ has units of inverse time. [If $h(t)$ were a delta function, representing a viscous medium, it would also have units of $(\text{time})^{-1}$.] Throughout the following analysis t_0 is included explicitly in order to preserve the correct units everywhere. Equation (6) is the proposed memory function that characterizes the dissipation arising from intergranular contacts.

III. SOLUTION OF THE WAVE EQUATION

Equation (5) is a linear, inhomogeneous wave equation that may be solved using standard techniques of Fourier analysis. First, on Fourier transforming both sides of the equation with respect to time, the convolution reduces to a product in the frequency domain, yielding

$$\left[1+j\omega\,\frac{(\frac{4}{3}\eta_f+\lambda_f)}{\rho_0 c_0^2}\,H(j\omega)\right]\frac{\partial^2\Psi(j\omega)}{\partial x^2}+k_0^2\Psi(j\omega) = -S\,\delta(x), \tag{7}$$

where $j=\sqrt{-1}$, ω is angular frequency, wave number $k_0=\omega/c_0$, and upper case letters H and Ψ are transforms of their lower case counterparts.

A second Fourier transform, with respect to distance, x, reduces Eq. (7) to an algebraic equation:

$$\left\{k_0^2-\left[1+j\omega\,\frac{(\frac{4}{3}\eta_f+\lambda_f)}{\rho_0 c_0^2}\,H(j\omega)\right]s^2\right\}\Psi_s=-S, \tag{8}$$

where the wave number s is the transform variable, and the subscript s denotes a transform with respect to x. From Eq. (8), the doubly transformed acoustic field may be written as

$$\Psi_s=\frac{S}{[q^2s^2-k_0^2]}, \tag{9}$$

where

$$q=\left[1+j\omega\,\frac{(\frac{4}{3}\eta_f+\lambda_f)}{\rho_0 c_0^2}\,H(j\omega)\right]^{1/2}. \tag{10}$$

The function $H(j\omega)$ is the temporal Fourier transform of the material response function, $h(t)$, in Eq. (6):

$$\begin{aligned}H(j\omega)&=\int_{-\infty}^{\infty}h(t)\exp-j\omega t\;dt\\&=t_0^{n-1}\int_0^{\infty}t^{-n}\exp-j\omega t\;dt\\&=\frac{\Gamma(1-n)}{(j\omega t_0)^{1-n}},\end{aligned} \tag{11}$$

where $\Gamma(\cdots)$ is the gamma function. The final expression in Eq. (11) is valid for $0<n<1$ but not for n identically equal to zero. It is demonstrated later, in Sec. V on pulse propagation, that if n were (incorrectly) put equal to zero, one consequence would be noncausal behavior in the form of acoustic arrivals before $t=0$. There is no such difficulty provided n, however small, is greater than zero.

With the result in Eq. (11), the radical in Eq. (10) becomes

$$q=[1+\chi_f(j\omega t_0)^n]^{1/2}, \tag{12}$$

where the various constants have been amalgamated into one-dimensionless loss coefficient:

$$\chi_f=\frac{(\frac{4}{3}\eta_f+\lambda_f)\Gamma(1-n)}{\rho_0 c_0^2 t_0}. \tag{13}$$

Equations (9) and (12) underpin the remainder of the discussion. Between them they offer the full solution to the propagation problem, provided the inversions back to the frequency and time domains can be performed.

IV. ATTENUATION AND DISPERSION

From Eq. (9) the frequency-dependent velocity potential is given by the inversion integral over wave number s:

$$\Psi(j\omega)=\frac{S}{2\pi q^2}\int_{-\infty}^{\infty}\left(s^2-\frac{k_0^2}{q^2}\right)^{-1}\exp jsx\;ds. \tag{14}$$

The poles of the integrand, $\pm k_0/q$, lie on either side of the real axis in the complex s plane, in the second and fourth quadrants when $\omega>0$ or the first and third quadrants if $\omega<0$. By integrating around a D in the upper and lower half-planes, respectively, for x positive and negative, the integral can be expressed explicitly:

$$\Psi(j\omega)=-\frac{jS}{2k_0 q}\exp-j\,\frac{k_0|x|}{q}, \tag{15a}$$

or, by substituting for q from Eq. (12) and using $k_0=\omega/c_0$,

$$\Psi(j\omega)=\frac{c_0 S}{2j\omega\sqrt{1+\chi_f(j\omega t_0)^n}}\exp-j\,\frac{\omega|x|}{c_0\sqrt{1+\chi_f(j\omega t_0)^n}}. \tag{15b}$$

According to Eqs. (15), each frequency component in the velocity potential field is an even function of x, as symmetry demands. Since the velocity potential is a real function of time, a further requirement is that $\Psi(j\omega)=\Psi^*(-j\omega)$, where the asterisk denotes a complex conjugate. This condition is clearly satisfied by Eq. (15b). Particular care is taken below to treat negative and positive frequencies correctly.

A standard way of representing the argument of the exponential function in Eq. (15b) is in terms of a complex wave number, k, which may be expressed in the form

$$k=\frac{\omega}{c_p}(1-j\beta), \tag{16}$$

where c_p is the (actual) phase speed of the compressional wave and the magnitude of the dimensionless loss tangent, β, is equal to $1/2Q$. Thus the velocity potential can be written as

$$\Psi=\Psi_0\exp-j\,\frac{\omega}{c_p}|x|\exp-\beta\,\frac{\omega}{c_p}|x|, \tag{17}$$

where Ψ_0 is the amplitude of the wave as given in Eq. (15b). By comparison of Eqs. (15b) and (17), the phase speed, c_p, is given by

$$c_p=c_0\,\mathrm{Re}[1+\chi_f(j\omega t_0)^n]^{1/2}, \tag{18}$$

and the loss tangent is

$$\beta=-\frac{c_p}{c_0}\,\mathrm{Im}[1+\chi_f(j\omega t_0)^n]^{-1/2}. \tag{19}$$

From Eq. (17) the attenuation coefficient, in nepers per unit length, is

$$\alpha_p = \frac{\omega}{c_p}\,\beta, \tag{20}$$

indicating that, if β and c_p were independent of frequency, then the attenuation would scale with the first power of frequency. Notice that in the absence of intergranular friction, when the coefficient χ_f is zero, q in Eq. (12) is real, and the attenuation coefficient vanishes. Another point to note is that β takes the same sign as ω, as shown below, and therefore α_p is always positive or zero, which is a necessary condition if the waveform in Eq. (17) is not to diverge. Equations (18) and (19) are generally valid expressions for the phase speed and attenuation in a medium with a memory of the form shown in Eq. (6).

Considering now the special case when n much less than unity, the term $(j\omega t_0)^n$ in the expressions for c_p and β may be approximated from the following argument. First,

$$[\mathrm{sgn}(\omega)j]^n = \cos(n\pi/2) + j\ \mathrm{sgn}(\omega)\sin(n\pi/2)$$

$$\approx 1 + \frac{jn\pi}{2}\ \mathrm{sgn}(\omega), \tag{21}$$

where, through the signum function sgn(..), explicit account has been taken of the sign of ω; and, second,

$$(|\omega|t_0)^n = \exp[n\ \ln(|\omega|t_0)] = 1 + n\ \ln(|\omega|t_0) + \cdots\ . \tag{22}$$

Hence, on expanding c_p and β [Eqs. (18) and (19)] in Taylor series to first order in the small parameter n, we arrive at the expressions

$$c_p \approx c_0\sqrt{1+\chi_f}\left[1 + \frac{n\chi_f}{2(1+\chi_f)}\ \ln(|\omega|t_0)\right]$$

$$= c_0\sqrt{1+\chi_f}\left[1 + \frac{2\beta_p}{\pi}\ \ln(|\omega|t_0)\right] \tag{23}$$

and

$$\beta \approx \beta_p\ \mathrm{sgn}(\omega), \tag{24a}$$

where the magnitude of β is

$$\beta_p = \frac{n\pi\chi_f}{4(1+\chi_f)}. \tag{24b}$$

The dispersive term in Eq. (23) is proportional to the frequency-independent loss tangent β_p, and is in complete agreement with O'Donnell *et al.*[20] and Horton,[19] who obtained an identical relationship between the c_p and β_p on the basis of the Kronig–Kramers relationships without considering a specific loss mechanism. Although β_p shows considerable variation between sediments (see Fig. 11), it usually takes a value in the range 0.001–0.02. The associated frequency dependence exhibited by the phase speed is very weak, falling between 0.015% and 3% per decade. In most circumstances this is entirely negligible, that is, the phase speed is satisfactorily approximated by the constant value

$$c_p = c_0\sqrt{1+\chi_f}. \tag{25}$$

However, as discussed later in Sec. VI, the dispersive term in the phase speed, although small, cannot be neglected when pulse propagation is being considered.

Equation (25) is an interesting result, which states that the presence of intergranular friction raises the wave speed above the value c_0 determined by the bulk modulus and bulk density of the medium [Eq. (3b)]. In effect, the friction at the intergrain contacts introduces some stiffness into the material, as a result of which the sound speed is increased. By comparing Eq. (25) with the expression for the compressional wave speed in an elastic medium, it is evident that the dissipation coefficient χ_f plays the role of a rigidity modulus. It must be emphasized, however, that the rigidity expressed in Eq. (25) is a purely frictional effect and is not associated with elastic rigidity of the material, which has been taken as zero.

Since the loss tangent β_p in Eq. (24) and the phase speed c_p in Eq. (25) are independent of frequency, it follows that, to this level of approximation, the attenuation coefficient, α_p, in Eq. (20) scales with the first power of frequency:

$$\alpha_p = \frac{|\omega|\beta_p}{c_p} = \frac{|\omega|n\pi\chi_f}{4c_0(1+\chi_f)^{3/2}}. \tag{26}$$

According to this result, intergranular friction gives rise to an attenuation that scales as the first power of frequency, and the associated logarithmic dispersion is expressed by Eq. (23). These features of the field are consistent with the observed geoacoustic properties of many unconsolidated marine sediments. Equation (26) in particular is a result we have been seeking, that is to say, an expression for the attenuation coefficient that matches the characteristic attenuation exhibited by saturated sediments. Two essential features of the theory give rise to this result: a dissipation term in the wave equation that takes account of hysteresis in the medium through a temporal convolution between a material memory function and the particle velocity [Eq. (1)]; and a specific form for the memory function that is characteristic of (dissipative) relaxation in granular media [Eq. (6)].

To establish the precision of Eqs. (24)–(26), consider the term $(\omega t_0)^n$, which is where the dependence on frequency originates in c_p and β [Eqs. (18) and (19)]. For a value of $n = 0.05$, which is representative of many sediments, the variation in $(\omega t_0)^n$ is 12% per decade of frequency. This small frequency dependence translates into an even weaker effect on the phase speed and the attenuation coefficient, as illustrated in Fig. 1, where the exact expressions for c_p and α_p in Eqs. (18)–(20) are plotted over 12 decades of the dimensionless frequency (ωt_0). For comparison, the approximate expressions in Eqs. (25) and (26) are included in the figure. The values of $n = 0.05$ and $\chi_f = 0.25$ used in generating these curves correspond to a medium-loss sediment (i.e., $\beta_p \approx 0.008$ or equivalently a bottom loss of 0.2 dB/m kHz). The exact curves are almost the same as the approximate forms over the huge frequency range in Fig. 1, confirming the validity of Eqs. (24)–(26) in predicting a loss tangent, β_p, that is independent of frequency, an attenuation coefficient, α_p, that scales with the first power of frequency, and a phase speed that shows a very low level of dispersion.

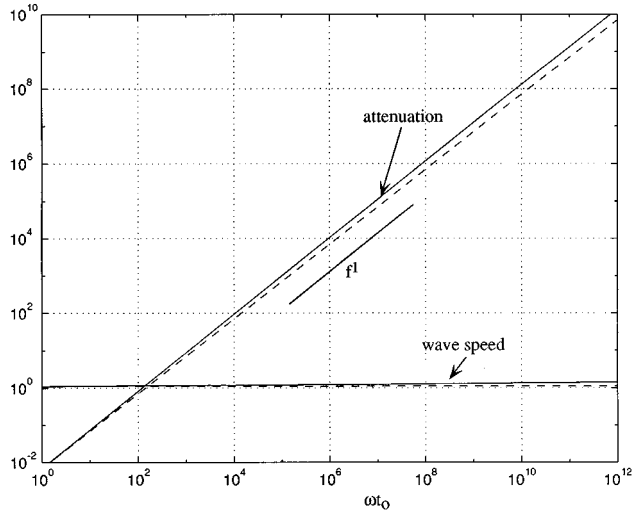

FIG. 1. Normalized attenuation ($\alpha c_0 t_0$) and phase speed (c/c_0) for a material showing intergranular friction. The solid lines are from the exact expressions in Eqs. (18)–(20) and the dashed lines are from the approximations in Eqs. (25) and (26). The curves were computed with $n=0.05$ and $\chi_f=0.25$, corresponding to $\beta_p \approx 0.008$.

V. OBSERVATIONS OF DISPERSION

Wingham[21] has reported a set of careful, laboratory measurements of compressional-wave dispersion and attenuation in gas-free, saturated medium sand. In his Fig. 4 he presents five data sets showing the relative change of phase speed over a frequency range from 100 to 350 kHz. Although he does not state it explicitly, the dispersion he observed in each case is easily calculated by reading from his curves: 1.27%, 0.81%, 1.00%, 0.92%, and 1.08%, the mean of which is 1.02%, per decade of frequency.

The attenuation that Wingham measured in the material scales with the first power of frequency, showing a loss tangent $\beta_p \approx 0.0065$ (equivalent to 0.16 dB/m kHz). When this value of β_p is substituted into our Eq. (23), the theoretically predicted dispersion is found to be 0.95% per decade, in close agreement with the mean value of 1.02% from Wingham's measurements. Dispersion at such a low level is very difficult to measure, especially *in situ*, which could account for the fact that it was not observed by other investigators.[17,18]

VI. PULSE PROPAGATION AND CAUSALITY

It has recently been demonstrated[37] that, in dealing with transient propagation in dissipative media, it is crucial to treat all frequency components accurately. This is especially true of the higher frequencies if the issue of causality is to be addressed, since it is they that govern the behavior of the pulse at short ranges and close to the origin in time.

The direct approach to obtaining the pulse shape in an unconsolidated sediment would be to perform a Fourier frequency inversion of the field expression in Eq. (17). However, with the exact versions of c_p and β in Eqs. (18) and (19), the Fourier integral is difficult to evaluate. On the other hand, if the high-precision approximations, c_p and β_p in Eqs. (24) and (25), are used instead, the integral becomes tractable but the resulting pulse is noncausal. This violation of causality arises directly from neglecting the tiny dispersive component in Eq. (25) in the Fourier inversion. The subtlety of the characteristic attenuation is well illustrated by this behavior.

To develop a satisfactory solution for the pulse shape, we return to the expression for the doubly transformed field in Eq. (9):

$$\Psi_s = -\frac{Sc_0^2}{\omega^2 - s^2\chi_f(j\omega t_0)^n - s^2 c_0^2}, \tag{27}$$

where q has been expressed explicitly. The procedure now is to reverse the order of the Fourier inversions by performing the integration over frequency first, to obtain the time-dependent field associated with each wave number. The inversion integral is

$$\psi_s(t) = \frac{1}{2\pi}\int_{-\infty}^{\infty} \Psi_s \exp j\omega t \, d\omega$$

$$= -\frac{Sc_0^2}{2\pi}\int_{-\infty}^{\infty} \frac{\exp j\omega t}{\omega^2 - s^2\chi_f c_0^2 (j\omega t_0)^n - s^2 c_0^2}\, d\omega. \tag{28}$$

To evaluate this integral, it is necessary to know the positions of the poles in the integrand, which are given by the roots of the denominator. For the case of interest, in which $0<n\ll 1$, these roots may be determined from a simple perturbation analysis.

The equation to be solved is

$$\omega^2 - s^2\chi_f c_0^2 (j\omega t_0)^n - s^2 c_0^2 = 0. \tag{29}$$

As a zero-order solution, let n be set identically equal to zero, even though the Fourier transform in Eq. (11) is invalid under this condition. Then Eq. (29) has two real roots, $\pm\omega_0$, where

$$\omega_0 = |s| c_0 \sqrt{1+\chi_f} = |s| c_p . \tag{30}$$

Since these poles lie on the real axis, it is evident that, with $n=0$, the inversion integral in Eq. (28) is noncausal in that it predicts acoustic arrivals at times t less than zero. Such nonphysical behavior is perhaps to be expected in view of the breakdown of Eq. (11) when $n=0$.

However, when n is finite but small compared with unity Eq. (11) is valid and, as shown below, the difficulty with noncausal arrivals vanishes. Under this condition, the two roots of Eq. (29) are displaced slightly from $\pm\omega_0$ on the real axis to positions $\omega_\pm$ in the complex ω plane. Taking just the leading-order terms in their real and imaginary parts, these complex roots are

$$\omega_\pm = \pm\omega_0 + jn\,\frac{\pi s^2 c_0^2 \chi_f}{4\omega_0}, \tag{31}$$

a result that is based on the approximations

$$(\pm j)^n = 1 \pm \frac{jn\pi}{2} \quad \text{and} \quad (\omega_0 t_0)^n = 1, \tag{32}$$

which are valid for $0<n\ll 1$. It is clear from Eq. (31) that, with n small but finite, both poles lie in the upper half of the complex ω plane, one in the first quadrant (ω_+) and the other symmetrically placed in the second quadrant (ω_-).

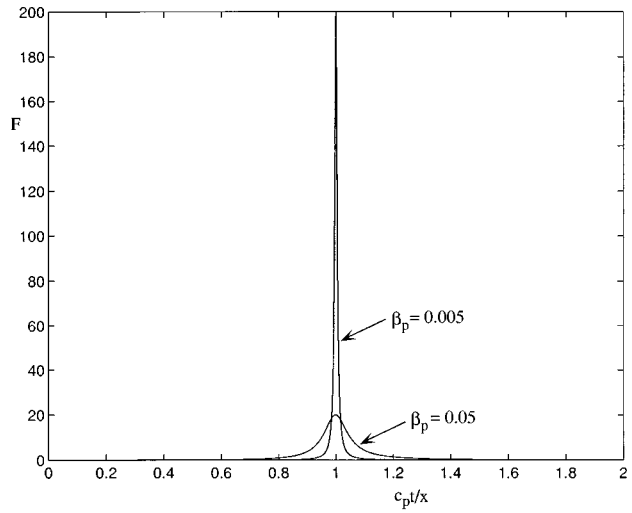

FIG. 2. Normalized velocity pulse, F, in a material showing intergranular friction, for two values of the (frequency-independent) loss parameter, β_p. The curves were computed from Eq. (39).

The inversion integral in Eq. (29) can now be expressed in the form

$$\psi_s(t) = -\frac{Sc_0^2}{2\pi}\int_{-\infty}^{\infty}\frac{\exp j\omega t}{(\omega-\omega_+)(\omega-\omega_-)}\,d\omega, \tag{33}$$

and evaluated directly. For positive times the integration contour must be around the top half-plane, in order to achieve convergence, and for negative times it is around the bottom half-plane. According to Eq. (31) there are no poles in the bottom half-plane, which immediately yields the result

$$\psi_s(t) = -\frac{jSc_0^2}{(\omega_+-\omega_-)}[e^{j\omega_+ t}-e^{j\omega_- t}], \quad t\geqslant 0$$
$$= 0, \quad t<0. \tag{34}$$

Thus every wave number component in the pulse, and hence the pulse itself, is causal. By recognizing that the poles do not lie precisely on the real axis, the difficulty with causality has been removed.

On substituting for the poles $\omega_\pm$ from Eq. (31), the expression in Eq. (34) becomes

$$\psi_s(t) = u(t)Sc_0^2\exp\left(-\frac{n\pi s^2 c_0^2\chi_f}{4\omega_0}\,t\right)\frac{\sin\omega_0 t}{\omega_0}, \tag{35}$$

where $u(t)$ is the unit step function. The particle velocity is obtained directly from Eq. (35) by performing the remaining Fourier inversion integral over wave number:

$$v(t,x) = -\frac{\partial\psi}{\partial x} = -\frac{1}{2\pi}\int_{-\infty}^{\infty} js\psi_s(t)\exp jsx\,ds. \tag{36}$$

With the aid of the expression for ω_0 in Eq. (30), this integral can be written as

$$v(t,x) = u(t)\frac{Sc_0^2}{\pi c_p}$$
$$\times\int_0^{\infty}\exp(-\beta_p sct)\sin(sc_p t)\sin(sx)ds, \tag{37}$$

where the loss tangent β_p and the phase speed c_p are given, respectively, by the frequency-independent expressions in Eqs. (24) and (25). Notice that the velocity field is an odd function of x, in accordance with the symmetry of the problem.

On recognizing that the integrand in Eq. (37) can be expressed as the sum of four exponentials, the integration can be performed directly to yield the shape of the velocity pulse:

$$v(t,x) = u(t)\frac{Sc_0^2}{2\pi c_p}\left\{\frac{\beta_p c_p t}{\beta_p^2 c_p^2 t^2+(c_p t-x)^2}\right.$$
$$\left.-\frac{\beta_p c_p t}{\beta_p^2 c_p^2 t^2+(c_p t+x)^2}\right\}$$
$$= u(t)\frac{Sc_0^2}{2\pi c_p x}F\left(\frac{c_p t}{x}\right), \tag{38}$$

where F is the dimensionless function

$$F(y) = \frac{\beta_p y}{(\beta_p y)^2+(y-1)^2}-\frac{\beta_p y}{(\beta_p y)^2+(y+1)^2}. \tag{39}$$

At $t=0$ the velocity waveform and its first derivative with respect to time are both zero. The velocity pulse is a sharply peaked function, as illustrated in Fig. 2 for two values of the loss tangent β_p. With decreasing β_p, the pulse grows taller and narrower, until in the limit of zero dissipation ($\chi_f=0$) it becomes a delta function. Formally, this limiting behavior may be derived with the aid of the identity

$$\lim_{a_1\to 0}\left\{\frac{a_1}{a_1^2+a_2^2}\right\} = \pi\delta(a_2), \tag{40}$$

from which it follows that

$$\lim_{\beta_p\to 0} v(t,x) = \frac{Sc_0}{2}\,\delta(c_0 t-x). \tag{41}$$

This is the correct retarded solution for propagation in a lossless medium. Notice that the velocity pulse in the presence of loss is not a retarded solution, since it varies with x and t individually and not just as $(c_p t-x)$.

The pressure pulse in the granular medium is derived from the velocity pulse by turning to the equation of motion [Eq. (1)], which includes the loss term representing intergranular friction. Although it is possible to derive an expression for the pressure from Eq. (1), the presence of the loss term complicates the analysis significantly. Rather than pursue lengthy algebra, the simple point is made that, since the velocity is causal, the pressure from Eq. (1) is also perfectly well-behaved.

VII. PORE-FLUID VISCOSITY?

It has been suggested by several authors that, in addition to intergranular friction, saturated porous materials such as marine sediments may exhibit viscous losses associated with local and global motions of the pore fluid.[5,27] The following

analysis is presented as an exploratory investigation of the significance of viscosity vis-à-vis intergranular friction in an unconsolidated sediment.

To account for local and global viscous dissipation, the linear equation of motion in Eq. (1), representing saturated sediments exhibiting only intergranular friction, must be modified by the addition of viscous loss terms. In fact, if the effects of local and global losses on wave propagation are assumed to be indistinguishable, a single viscous term is sufficient, allowing the equation of motion for the saturated medium to be written as

$$\rho_0 \frac{\partial v}{\partial t} + \frac{\partial p}{\partial x} - \left(\frac{4}{3}\,\eta_f + \lambda_f\right) \frac{\partial^2 [h(t) \otimes v(t)]}{\partial x^2} - \left(\frac{4}{3}\,\eta + \lambda\right) \frac{\partial^2 v}{\partial x^2} = 0, \tag{42}$$

where the material response function, $h(t)$, is as defined in Eq. (6) and η, λ are the shear and bulk viscosities, respectively, of the pore fluid. It is implicit in Eq. (42) that the viscosity is being regarded as a bulk property of the material, in the same spirit as in the previous treatment of the intergranular friction.

Conservation of mass [Eq. (2)] and the equation of state [Eq. (3)] are unaffected by the dissipation and hence the wave equation is

$$\frac{\partial^2 \psi}{\partial x^2} - \frac{1}{c_0^2} \frac{\partial^2 \psi}{\partial t^2} + \frac{(\frac{4}{3}\,\eta_f + \lambda_f)}{\rho_0 c_0^2} \frac{\partial^3 [h(t) \otimes \psi(t)]}{\partial t\, \partial x^2} + \frac{(\frac{4}{3}\,\eta + \lambda)}{\rho_0 c_0^2} \frac{\partial^3 \psi}{\partial t\, \partial x^2} = -S\,\delta(t)\,\delta(x), \tag{43}$$

where ψ is the velocity potential [Eq. (5)]. It is convenient to amalgamate the two loss terms into one, as follows:

$$\frac{\partial^2 \psi}{\partial x^2} - \frac{1}{c_0^2} \frac{\partial^2 \psi}{\partial t^2} + \frac{(\frac{4}{3}\eta_f + \lambda_f)}{\rho_0 c_0^2} \frac{\partial^3 [\tilde{h}(t) \otimes \psi(t)]}{\partial t \partial x^2} = -S\,\delta(t)\,\delta(x), \tag{44}$$

where the modified material response function, identified by the tilde, is

$$\tilde{h}(t) = b\,\delta(t) + h(t), \quad \text{and} \quad b = \frac{(\frac{4}{3}\eta + \lambda)}{(\frac{4}{3}\eta_f + \lambda_f)}. \tag{45}$$

Clearly, when the relative loss coefficient, b, is zero, corresponding to an absence of viscosity, the linear wave equation in Eq. (44) reduces to the form appropriate to materials exhibiting only intergranular friction [Eq. (5)].

By analogy with Eq. (15a), the solution of Eq. (44) for the frequency dependence of the field may be written immediately as

$$\Psi(j\omega) = -\frac{jS}{2k_0 \tilde{q}} \exp -j\,\frac{k_0 |x|}{\tilde{q}}, \tag{46}$$

where

$$\tilde{q} = \left[1 + j\omega\,\frac{(\frac{4}{3}\eta_f + \lambda_f)}{\rho_0 c_0^2}\,\tilde{H}(j\omega)\right]^{1/2} = [1 + (j\omega t_0)\xi + \chi_f (j\omega t_0)^n]^{1/2}; \quad 0 < n \ll 1. \tag{47}$$

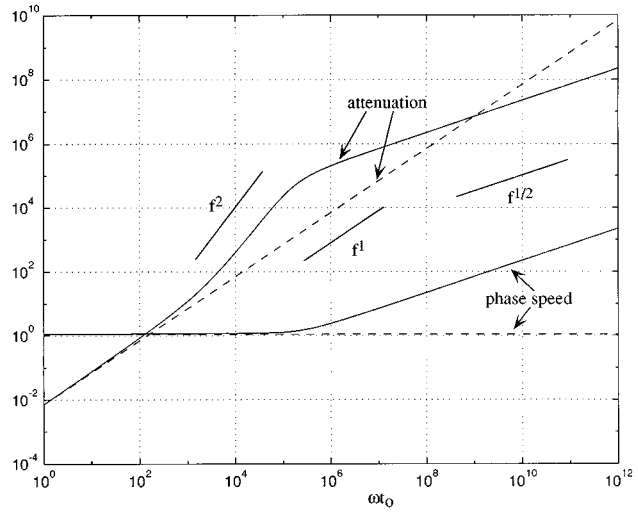

FIG. 3. Normalized attenuation ($\alpha c_0 t_0$) and phase speed (c/c_0). The solid lines, computed from Eqs. (50) to (52) with $\chi_f = 0.25$, $\xi = 10^{-5}$, and $n = 0.05$, corresponding to $\beta_p \approx 0.008$ and $b \approx 4 \times 10^{-5}$, represent a material showing both intergranular friction and viscosity. For reference the dashed lines, from Fig. 1, show the effects of intergranular friction alone.

In these expressions, the temporal Fourier transform of $\tilde{h}(t)$ is

$$\tilde{H}(j\omega) = b + \frac{\Gamma(1-n)}{(j\omega t_0)^{1-n}}, \tag{48}$$

the coefficient ξ representing viscous losses is

$$\xi = \frac{(\frac{4}{3}\eta_f + \lambda_f) b}{\rho_0 c_0^2 t_0} = \frac{b}{\Gamma(1-n)}\,\chi_f, \tag{49}$$

and χ_f, the coefficient for intergranular friction, is as defined in Eq. (13). The phase speed of the wave is

$$\tilde{c}_p = c_0\ \mathrm{Re}(\tilde{q}) = c_0\ \mathrm{Re}[1 + (j\omega t_0)\xi + \chi_f (j\omega t_0)^n]^{1/2} \tag{50}$$

and the attenuation coefficient is

$$\tilde{\alpha}_p = \frac{\omega}{\tilde{c}_p}\,\tilde{\beta}, \tag{51}$$

where

$$\tilde{\beta} = -\frac{\tilde{c}_p}{c_0}\,\mathrm{Im}\left(\frac{1}{\tilde{q}}\right) = -\frac{\tilde{c}_p}{c_0}\,\mathrm{Im}[1 + (j\omega t_0)\xi + \chi_f (j\omega t_0)^n]^{-1/2} \tag{52}$$

is the loss tangent.

Figure 3 shows the phase speed and the attenuation coefficient from Eqs. (50) to (52) as a function of the dimensionless frequency ωt_0. At the lower frequencies, where intergranular friction is the dominant loss mechanism, the attenuation varies linearly with the first power of frequency. However, at intermediate and high frequencies viscosity dominates and the attenuation scales with f^2 and $f^{1/2}$, respectively, as in a viscous fluid. The transition frequency, where the predominant form of loss switches from intergranular friction to viscosity of the pore fluid, depends on the magni-

tude of the relative loss parameter b, defined in Eq. (45). In addition to modifying the attenuation, the presence of viscosity introduces relatively high dispersion, which varies with frequency as $f^{1/2}$ in the higher-frequency, viscous regime.

With the parameters used to generate Fig. 3 ($n=0.05$, $\chi_f=0.25$, and $\xi=10^{-5}$), the effects of viscosity are apparent in the attenuation when the dimensionless frequency ωt_0 is greater than several hundred and in the phase speed when $\omega t_0>10^5$. If ξ were increased, representing higher viscosity, the effects of viscous losses on the attenuation and phase speed would cut in at lower frequencies. A smaller value of ξ, corresponding to lower viscosity, would shift the transition frequency upward. It is interesting that at high frequencies ($\omega t_0>10^9$ in Fig. 3) the attenuation due to the combined effect of intergranular friction and viscosity is actually less than that due to friction alone. At these frequencies the viscosity does not have an additive effect on the attenuation but acts as though intergranular friction were absent, even though the two types of dissipation are represented by additive terms in the wave equation. Even if it existed in real materials, however, this reduced high-frequency attenuation, falling below the f^1 curve for intergranular friction, may not be observable because of the onset of other loss mechanisms, notably scattering.[38]

In fact, in real saturated marine sediments the question of whether pore-fluid viscosity has any detectable effect on the attenuation is not entirely resolved. If it were significant then, according to Eq. (50), it should also introduce an appreciable level of dispersion, that is, a level much higher than that due to intergranular friction alone (Fig. 3). However, the experiments of Wingham,[21] in which he measured the attenuation and dispersion in saturated medium sand up to a frequency of 350 kHz, are entirely consistent with the presence of intergranular friction, but show no evidence of effects due to pore fluid viscosity. As discussed in Sec. V, Wingham found an attenuation that scaled with the first power of frequency, and weak logarithmic dispersion characteristic of intergranular friction, not the relatively strong dispersion, varying as $f^{1/2}$, that would be indicative of viscosity.

The absence of dispersion reported by Hamilton[18] also militates against pore-fluid viscosity as a significant loss mechanism in saturated marine sediments. Moreover, in a discussion of attenuation in sandstone saturated with water, White[13] concludes that losses due to fluid viscosity are entirely negligible. On the other hand, in very early measurements on earth materials, Born[39] found that the attenuation in bars of dry shale, limestone, and sandstone was proportional to the first power of frequency, but when small quantities of water were added the power law changed to f^m, where the exponent m lay between 1 and 2, which may have been due to viscous dissipation. As far as unconsolidated marine sediments are concerned, however, the weight of evidence points to the conclusion that pore-fluid viscosity is negligible and that the dissipation is governed by intergranular friction. Accordingly, viscous losses are excluded from the remainder of the discussion.

VIII. WOOD'S EQUATION FOR c_0

A sediment is a two-phase medium consisting of loose mineral grains and seawater. In the absence of dissipation at the grain-to-grain contacts, the wave speed in such a medium would be given by Wood's equation[40] in terms of weighted means of the bulk moduli and densities of the two constituents of the material. In other words, Wood's equation can be used to express the sound speed c_0 as a function of known mechanical properties of the mineral grains and the seawater.

As given in Eq. (3b), the sound speed in the absence of friction between mineral grains depends on the bulk modulus, κ, and bulk density, ρ_0, of the sediment:

$$c_0=\sqrt{\frac{\kappa}{\rho_0}}. \tag{53}$$

Now, the density ρ_0 is the weighted mean

$$\rho_0=N\rho_w+(1-N)\rho_g, \tag{54}$$

where N is the porosity of the medium and the densities of seawater and mineral grains are, respectively, $\rho_w=1024\ \mathrm{kg/m^3}$ and $\rho_g=2700\ \mathrm{kg/m^3}$. Similarly the bulk modulus of the sediment is given by the mean

$$\frac{1}{\kappa}=N\,\frac{1}{\kappa_w}+(1-N)\,\frac{1}{\kappa_g}, \tag{55}$$

where $\kappa_w=2.25\times10^9$ Pa is the bulk modulus of the pore water. A reasonable value for the bulk modulus of the mineral grains is $\kappa_g=1.47\times10^{10}$ Pa, which is the geometric mean of values reported by Stoll[27] (3.6×10^{10} Pa) and Chotiros[41,42] (6×10^9 Pa). By combining Eqs. (53)–(55), the expression for c_0 becomes

$$c_0=\sqrt{\frac{\kappa_w\kappa_g}{[N\rho_w+(1-N)\rho_g][N\kappa_g+(1-N)\kappa_w]}}, \tag{56}$$

which is Wood's equation for the sound speed in the sediment in the absence of intergranular friction.

Equation (56) is a useful result in that it links an important wave parameter, c_0, with a measurable mechanical property of the sediment, the porosity N. In passing, it is emphasized that Wood's equation is not appropriate for estimating the actual wave speed, c_p, in a sediment, since it takes no account of intergranular friction in the material. In fact, Hamilton[43,44] compared Wood's equation with measurements of wave speed versus porosity and found little correspondence between the data and the theoretical expression. An extension of Wood's theory was developed by Gassmann,[13,45,46] who included a frame bulk modulus in his argument. Although Gassmann's approach may be relevant to rigid, porous media such as rocks, which possess a skeletal elastic frame, it is difficult to see how it could apply to unconsolidated marine sediments.

IX. RANDOM-PACKING, ROUGH-PARTICLE MODEL OF SEDIMENTS

Hamilton[18,47] has measured correlations between wave properties (sound speed and attenuation) and mechanical properties (density, porosity, and grain size) of surficial marine sediments. To establish the corresponding theoretical re-

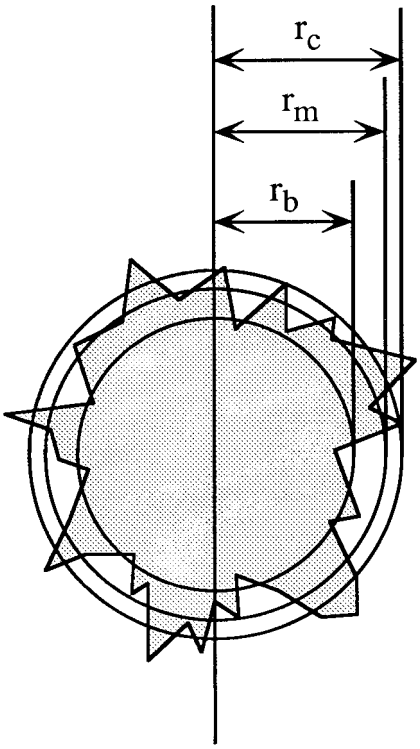

FIG. 4. Schematic of a rough sediment particle. The body radius, r_b, is a measure of the particle size in the absence of the rough surface. The contact radius, r_c, is the effective size of the particle, controlling the packing density in the sediment; and the mean radius, r_m, is intermediate between r_c and r_b. The mean grain diameter of a sediment is identified as $u_g = 2r_b$.

lationships, it is necessary to identify connecting links between the following: (1) density and porosity; (2) intergranular friction and grain size; and (3) porosity and grain size. The first of these pairings is already known and is given by Eq. (54), while the second derives from a simple model of elastic bodies in contact, as discussed below in Sec. XI. The remaining link, between porosity and grain size, which also couples density to grain size through Eq. (54), is now developed on the basis of a random-packing model of the sediment.

Particle roughness plays a central role in the argument, since it is an important factor in determining the porosity and the density of all sediments. To model the porosity, the mineral particles constituting the sediment are treated as rough spheres of uniform size, as illustrated purely schematically in Fig. 4. Measured from the centroid, r_m is the radius of a smooth sphere of volume equal to that of the particle itself. The inner radius, $r_b < r_m$, provides a measure of the body size of the particle, and corresponds approximately to the radius of the sphere that would remain after polishing off the rough surface. The outer radius, $r_c > r_m$, represents the contact radius, that is, on average $2r_c$ is the closest possible approach between the centers of two adjacent sediment grains. According to this description, the roughness prevents the mean surfaces of the particles from making contact, keeping them separated by a finite distance, which, on average, is equal to $2(r_c - r_m)$.

For a sediment in which each grain is in close contact with the surrounding grains, the porosity is the volume fraction of sea water in the medium, which can be expressed as

$$N = 1 - P, \tag{57}$$

where P is the average volume of contiguous grains per unit volume. In the absence of surface roughness, that is, if the grains were smooth spheres, P would be the packing factor, whose value depends on the packing arrangement. For spheres of uniform size, the packing factor is $P = \pi/6 = 0.52$ for simple-cubic symmetry, $P = 0.68$ for a body-centered cubic arrangement, or $P = 0.74$ for both face-centered cubic and hexagonal close-packed structures.[48]

However, for a random packing of smooth spheres, which is more appropriate to sediment particles than any of the regular packing structures, the packing factor has been observed experimentally[49] to be 15% less than the maximum possible value of 0.74 achieved with either of the two close-packed arrangements. Thus a random packing of smooth spheres is described by $P = 0.63$, which is the value adopted for the packing factor of sediment particles in the following discussions. Note that the porosity of a sediment consisting of smooth spherical particles of uniform size would be independent of the sphere radius regardless of the packing arrangement, but in practice such behavior is not observed: The porosity of sediments depends quite strongly on particle size.[18,47]

When the roughness of the spheres is taken into account (Fig. 4), a simple geometrical argument shows that the expression in Eq. (57) for the porosity must be modified as follows:

$$N = 1 - P\,\frac{r_m^3}{r_c^3} = 1 - P\left\{\frac{u_g + 2\Delta}{u_g + 4\Delta}\right\}^3, \tag{58}$$

where $P = 0.63$ is still the packing factor for a random arrangement of smooth spheres of uniform size, and $u_g = 2r_b$ is the body diameter, which is identified with reported measurements of particle size. In formulating Eq. (58), the excursions of the roughness about the mean radius, r_m, have been treated as symmetrical (i.e., the skewness of the distribution is zero). Thus the roughness is characterized by a single statistical parameter, $\Delta = (r_c - r_m) = (r_m - r_b)$, which is identified as the rms roughness height relative to the mean.

If Δ scaled with the body diameter, u_g, then the porosity according to Eq. (58) would still be independent of particle size, which is not a characteristic of real sediments. As shown in Fig. 5, Eq. (58) matches reported porosity versus grain size data[18,47,50] when Δ is taken to be a constant (independent of particle size, u_g) with a value $\Delta = 3\ \mu$m. It can be seen in Fig. 5 that the measurements of sediment porosity decrease with increasing grain size.[18,47,50] The finest-grained materials (clays) show the highest porosity, in the region of $N \approx 0.9$, with the coarse sands exhibiting the lowest value of $N \approx 0.37$. These extreme values of porosity, as observed in actual sediments, correspond to two distinct physical situations. They emerge naturally from Eq. (58), and interestingly enough neither depends on the magnitude of the rms roughness, Δ.

In the limit of large particle size ($u_g \to \infty$), the minimum porosity from Eq. (58) is given by

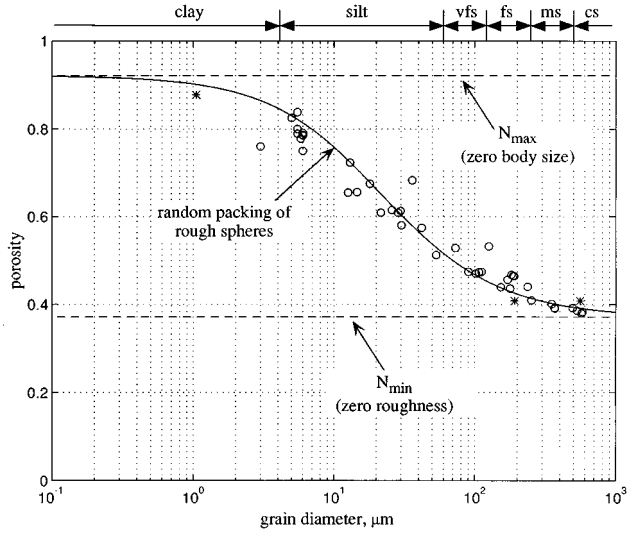

FIG. 5. The porosity as a function of grain diameter. The solid line is from Eq. (58) with $\Delta = 3\ \mu$m and $P = 0.63$; and the dashed lines represent the extreme cases in Eqs. (59) and (60). The symbols are data for saturated marine sediments from: (○), Hamilton (Refs. 18, 47); (*), Richardson and Briggs (Ref. 50). The key to the sediment type is: cs=coarse sand; ms=medium sand; fs=fine sand; vfs=very fine sand.

$$N_{\min} = 1 - P = 0.37, \tag{59}$$

which, physically, corresponds to a random packing of smooth spheres, representative of coarse sand grains whose rms roughness is negligible relative to the body size. At the other extreme of small particle size ($u_g \to 0$), the maximum porosity obtained from Eq. (58) is

$$N_{\max} = 1 - \frac{P}{8} = 0.92, \tag{60}$$

which is characteristic of clay particles that are, in effect, all roughness with zero body size. Between the outer and inner size scales represented by Eqs. (59) and (60), respectively, the shape of the porosity versus grain-size curve does, of course, depend on the magnitude of the roughness, Δ. It can be seen in Fig. 5 that, with the rms roughness set to $\Delta = 3\ \mu$m, as cited above, Eq. (58) provides a very good match to the data in the figure over three decades of grain size. This is an important observation, in view of the fact that the rough, random-packing model is such a simple, one-parameter treatment of sediments. Naturally, it would be desirable to corroborate the size-independent roughness hypothesis, as well as the rms roughness scale, but an independent check is difficult because very few direct measurements of particle roughness have been reported in the literature.

Figures 6 and 7, respectively, show the density versus porosity from Eq. (54) and the density against grain diameter from Eqs. (54) and (58). Included in the figures are measurements of porosity, density, and grain size made by Hamilton,[18,47] and Richardson and Briggs[50] on a large number of surficial sedimentary materials ranging from coarse sand to clay. As with the porosity versus grain size (Fig. 5), the rough-particle, random-packing model of sediments provides a sensible description of the relationship between density and grain size over a range of particle diameters spanning about three decades (clays to coarse sand). Note that the model is based purely on geometry, suggesting that, in surficial sediments, electrostatic and physico-chemical interactions between particles are of little importance in determining the porosity and density of the medium.

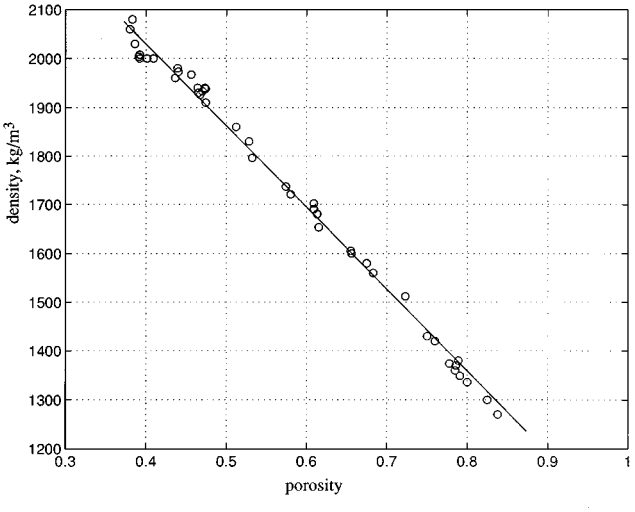

FIG. 6. Plot of density against porosity. The symbols represent data from Hamilton (Refs. 18, 47) and the solid line is the expression in Eq. (54).

If it were not for the fact that it works so well, the unified treatment of sediments embodied in the rough-sphere model may appear to be unduly ambitious. Conventionally, clays, in which the mineral particles are elongated platelets[18] with a very high aspect ratio, are considered to be fundamentally different in structure from the silts and sands, whose grains conform much more closely to the spherical model. Thus although it is reasonable that the rough-sphere model should be representative of the porosity and density of sands and silts, there is a question as to why should it also be applicable to clays?

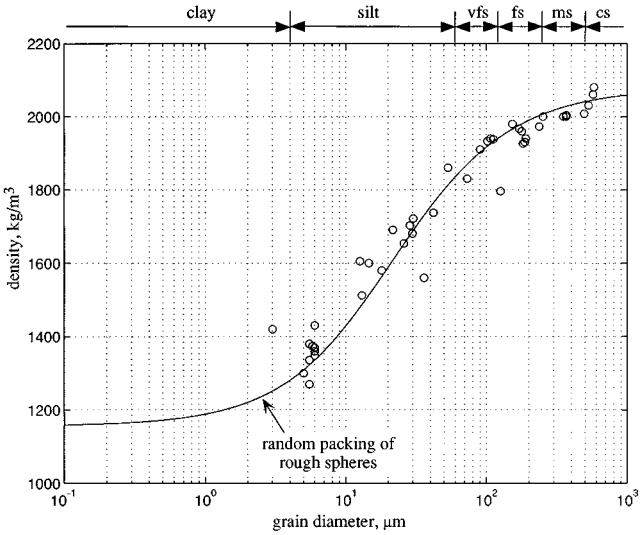

FIG. 7. Sediment density as a function of mean grain diameter. The curved line is from Eqs. (54) and (58), and the symbols represent data from Hamilton (Refs. 18, 47). The key to the sediment type is: cs=coarse sand; ms=medium sand; fs=fine sand; vfs=very fine sand.

In defence of the unified treatment of sediments represented by Eq. (58), the issue of clays is interpreted as follows. It is argued that the geometry of the mineral particles in clay is, in fact, not fundamentally different from that of sand or silt grains. A clay platelet may be thought of as a special, if rather extreme, case of the spherical geometry shown in Fig. 4, in which the body size is much smaller than the rms roughness, Δ. Under this condition, the inherently spherical shape of the particle vanishes, leaving only the roughness, which, if it were to conform to the diagram in Fig. 4, would be statistically isotropic (i.e., the rms roughness would be the same in all radial directions). But a clay platelet is clearly not isotropic. However, if the platelets were randomly orientated in the medium, as they probably are in surficial sediments, given the nature of the depositional process, the effect on the packing structure would be essentially the same as if the individual particles had an isotropic roughness. This would account for the fact that the porosity of surficial clays, like that of the sands and silts, is well represented by the rough-sphere model.

To depths of half a meter or more in the sediment, the porosity of sands and silts is more or less constant, but that of clays tends to decrease by perhaps 10% relative to the surficial value.[51] Such a reduction in porosity of the clays would appear to be at odds with the rough-sphere model [Eq. (58)], since the clay particles half a meter or so beneath the surface are presumably the same size as those at the seawater–sediment interface. The deeper particles, however, may have settled into an arrangement which is no longer isotropic but shows a degree of particle alignment. Even mild polarization would reduce the average center-to-center distance and thus decrease the porosity. Although the rough-sphere model in Fig. 4 could be adapted to account for some anisotropy in the packing structure of the deeper clay particles, this is beyond the scope of the present discussion.

X. POROSITY AND A BI-MODAL GRAIN SIZE DISTRIBUTION

The rough-sphere model as it appears in Eq. (58) is representative of sediments in which the grain-size distribution is unimodal, that is, the particles are fairly uniform in size. As illustrated in Fig. 5, many marine sediments are indeed characterized by a single grain size, but not all. In some sediments, especially the finer silts and the clays, the particle size distribution is bimodal (or perhaps multimodal), the effect of which is to lower the porosity and raise the density of the medium relative to the values that would be observed in the presence of the larger particles alone.[51] For such a sediment, Eq. (58) may be expected to fail.

However, a minor modification to the formulation in Eq. (58) allows for the effect of an admixture of smaller particles on the porosity of the medium. Assuming that the smaller particles simply in-fill the pore spaces formed between the larger grains, that is, they displace their own volume of pore water but have no effect on the random-packing structure of the larger particle species, then the expression for the porosity becomes

$$N = 1 - P\left\{\frac{u_g + 2\Delta}{u_g + 4\Delta}\right\}^3 (1+\gamma), \tag{61}$$

where γ is the volume ratio of the smaller to the larger grain species and u_g is now the mean diameter of the larger grains in the sediment. The remaining symbols in Eq. (61) take the same values as in Eq. (58). To obtain the density of the bimodal sediment, Eq. (61) is substituted into the weighted mean in Eq. (54). Clearly, when $\gamma = 0$, corresponding to a unimodal particle size distribution, Eq. (61) reduces identically to Eq. (58).

Occasionally, a value for γ is reported, along with other geoacoustic data, for sediments with a known bimodal grain-size distribution. For example, γ may be cited indirectly as a percentage of clay in a predominantly silty material. Obviously, γ will never be large enough to make N negative, although in high porosity materials γ may be greater than unity. All the sands exhibit a porosity that is relatively low ($N \leqslant 0.6$), and in these materials the effect of a secondary, in-filling particle species is usually negligible, that is, $\gamma = 0$. This, however, is definitely not the case in some of the silts and the clays, where in-filling of pore space by smaller particles may reduce the porosity and increase the density significantly. For such sediments, it is important to use an appropriate value of γ when estimating the porosity and density of the medium, especially if the model were being used as the basis of a geoacoustic inversion. Having said this, our attention will be focused throughout the remainder of the present discussion on sediments with a unimodal grain-size distribution, for which γ is zero and Eq. (58) holds.

XI. INTERGRANULAR FRICTION AND PARTICLE SIZE

To complete the description of unconsolidated sediments, a relationship must be established which couples the wave properties (sound speed and attenuation) to the mechanical parameters (porosity, density, and grain size). Taking intergranular friction as being the fundamental mechanism underlying wave behavior, and grain size as the independent variable characterizing the mechanical structure of the sediment, the following fractional power-law relationship is proposed:

$$\chi_f = \frac{\mu_c}{\rho_0 c_0^2} = \left(\frac{u_g}{u_0}\right)^{1/3} \frac{\mu_0}{\rho_0 c_0^2}, \tag{62}$$

where u_g is the mean grain diameter (μm) and, as in the phi units of grain size, the reference grain diameter is chosen as $u_0 = 1000$ μm, corresponding to coarse sand. By substituting the first of the expressions in Eq. (62) into Eq. (25), it is clear that the coefficient μ_c is analogous to the rigidity modulus (one of the Lamé parameters) in elasticity theory, but only so far as determining the compressional wave speed is concerned. Thus μ_c is the compressional, frictional-rigidity modulus of the sediment. (As discussed in a later paper, a different frictional-rigidity modulus determines the shear wave speed.) According to Eq. (62), μ_c scales as the cube root of the grain size, the scaling factor being $\mu_0 = 2 \times 10^9$ Pa, which is a material-independent constant whose

value has been established on the basis of a best fit to wave speed versus grain size data (Fig. 8).

It may appear that two unknown parameters have been introduced in Eq. (62), μ_0 and u_0, but it should be clear that they are not independent and that in effect there is only one, namely $\mu_0/(u_0)^{1/3}=2\times10^8$ Pa/$(\mu\text{m})^{1/3}$. The formulation in Eq. (62) avoids the use of a scaling constant with the rather awkward units of pressure/(length)$^{1/3}$.

The expression in Eq. (62) should be valid even for a sediment with a bimodal particle distribution, provided that the smaller particle species merely in-fills the pores formed by the larger particles but plays no part in intergranular dissipation. In such a case, u_g would be the mean diameter of the larger grains.

Equation (62) is suggested by the Hertz theory of deformation of spherical, elastic bodies in contact.[52] When the spheres are pressed together under a force F, a circular area of contact forms with a radius, a, that is proportional to the sphere radius raised to the power of one third:

$$a=\sqrt[3]{\frac{3}{4}\frac{F(1-\sigma^2)}{E}R}, \tag{63}$$

where R is the radius of the spheres, which are taken to be of equal size, and (E,σ) are, respectively, Young's modulus and Poisson's ratio for the elastic material constituting the spheres. The maximum tensile stress acts radially around the circumference of the circle of contact. Taking the two spheres as being adjacent mineral grains in contact, Eq. (62) states that the coefficient of intergranular friction, χ_f, is proportional to the length of the line of highest tensile stress, a distance equal to $2\pi a$, which scales as the cube root of the grain size.

It is implicit in the Hertz theory that the two spherical particles are smooth bodies in contact, whereas in Sec. IX, the mineral grains have been treated as rough particles in the discussion of porosity. These two pictures of the mineral grains may be reconciled by imagining that, in the immediate vicinity of the points of contact, the geometry of the rough particles is locally spherical, suggesting that the cube-root scaling from the Hertz theory in Eq. (62) might be expected to apply. However, the magnitude of the interaction, as measured by the coefficient μ_0 in Eq. (62), is determined, not by the body radius of the particles, but from the rms roughness, that is, the average local radius of curvature at the point of contact, which is independent of grain size. Since a value for μ_0 does not emerge naturally from any available theory of particle-to-particle interaction, it can be determined only from a match to data, which is how the value cited above was obtained.

If Eq. (62) for χ_f as a function of grain size is accepted as a working hypothesis, the sound speed [Eq. (25)] and attenuation [Eq. (24b)] in the sediment take the forms

$$c_p=\sqrt{c_0^2+\left(\frac{u_g}{u_0}\right)^{1/3}\frac{\mu_0}{\rho_0}} \tag{64}$$

and

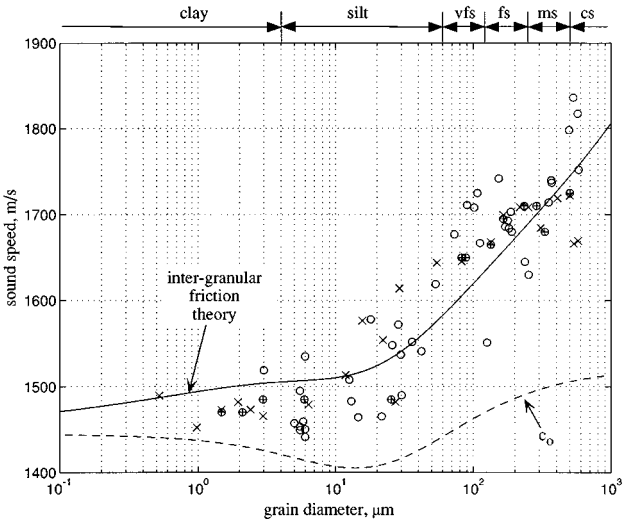

FIG. 8. Wave speed versus mean grain diameter, u_g. The symbols represent data published by Hamilton (Refs. 18, 47) (○), Richardson (Ref. 53) (⊕), and Richardson and Briggs (Ref. 54) (x) and the key to the sediment type is: cs=coarse sand; ms=medium sand; fs=fine sand; vfs=very fine sand. The solid line is c_p from Eq. (64), with c_0 and ρ_0 evaluated from Eqs. (54), (56), and (58). For comparison, the dashed line shows c_0.

$$\beta_p=\frac{n\pi}{4}\frac{u_g^{1/3}}{u_g^{1/3}+w}, \tag{65}$$

where

$$w=\frac{u_0^{1/3}\rho_0 c_0^2}{\mu_0}. \tag{66}$$

These expressions give the wave properties in terms of the grain size, which itself is related to the density, ρ_0, and the porosity, N, through Eqs. (54) and (58). [It should be borne in mind that c_0 is also a function of u_g, as given by Eqs. (56) and (58).] Thus all the parameters of the sediment have been expressed in terms of the grain size, through the simple algebraic expressions developed above.

XII. WAVE SPEED VERSUS MECHANICAL PROPERTIES

Figure 8 shows the wave speed, c_p, plotted as a function of the mean grain size, as evaluated from Eq. (64). The data represented by the symbols in this figure, and also in Figs. 9 and 10, are from tables of measured parameter values published by Hamilton,[18,47] Richardson,[53] and Richardson and Briggs.[54] The value for the scaling coefficient, $\mu_0=2\times10^9$ Pa, cited above in connection with Eq. (62) was obtained by matching the curve to the data in Fig. 8. Otherwise, there are no adjustable parameters available to facilitate the fit. Although there is some spread in the data, it is clear that the theory faithfully follows the trend of the measurements in Fig. 8 over a range of particle sizes spanning at least three decades, representing clays, silts, and all grades of sand. For comparison with c_p, the dashed line in Fig. 8 shows the sound speed, c_0, in the absence of friction, as evaluated from Eqs. (56) and (58).

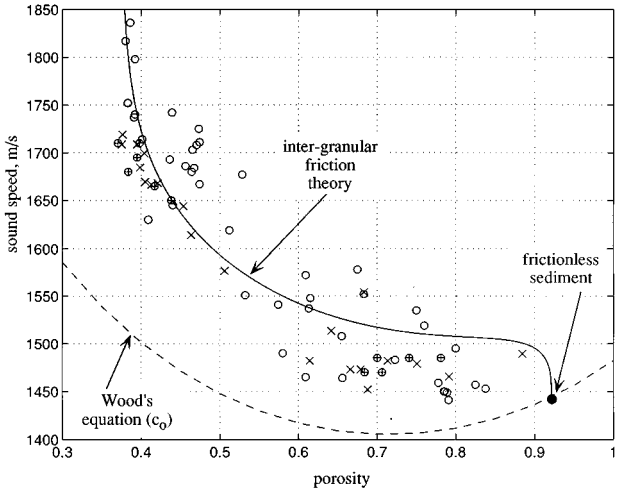

FIG. 9. Wave speed as a function of porosity. The solid line is a plot of Eq. (64) in conjunction with Eqs. (54), (56), and (58), and the symbols represent published data, as identified in the legend to Fig. 8. The dashed line is Wood's equation for c_0 in Eq. (56).

The sound speed versus porosity is shown in Fig. 9, where the solid line represents Eq. (64) in conjunction with Eqs. (54), (56), and (58). Again, the theory of intergranular friction can be seen to provide a very reasonable description of the data. For comparison, Wood's equation for c_0 [Eq. (56)] is included as the broken line in the figure. The only point of intersection of the two theoretical curves corresponds to the ultimate in fine-grained materials, that is to say, a (fictitious) sediment in which the particle (body) size approaches zero and intergranular friction is essentially absent. Elsewhere in the plot the two curves diverge fairly dramatically, but only Eq. (64) for c_p matches the data, thus illustrating the importance of intergranular friction in determining the sound speed in the sediment.

The predicted relationship between sound speed and density is compared with published data in Fig. 10. It can be seen that the solid line, representing Eq. (64) in conjunction with Eqs. (54), (56), and (58), passes through the measured points very nicely. In fact, it is evident from Figs. 8–10 that all the observed correlations between wave speed and the mechanical properties of many sediments are described reasonably by the equations developed in the previous sections. This is interesting for several reasons, not the least being that, with μ_0 and Δ fixed, there are no adjustable parameters in the theory to help match the individual curves to the data.

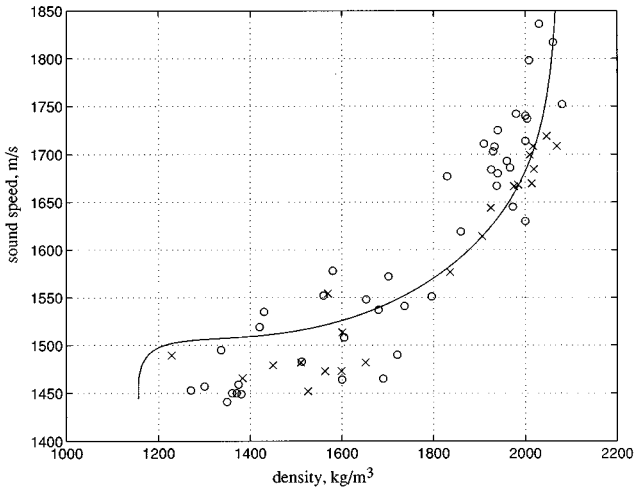

FIG. 10. Sound speed as a function of density. The curved line is a plot of Eq. (64) in conjunction with Eqs. (54), (56), and (58), and the symbols represent data published by Hamilton (Refs. 18, 47) (○), and Richardson and Briggs (Ref. 54) (x).

It is perhaps worth commenting on the spread in the data around the theoretical predictions in Figs. 8–10. The variability in the measurements may be partly due to experimental error, but other factors may also be at work. For instance, in some sediments the bulk modulus, κ_g, and the density, ρ_g, of the mineral particles could be different from the values used in evaluating the theory; and some of the data points in the figures may represent sediments with a bimodal particle size distribution (i.e., $\gamma \neq 0$). Factors such as these could be responsible for the multivalued behavior exhibited by the data in Figs. 8–10. If, for a specific sediment, information is available on the properties of the mineral particles or on the size distribution, it should be used as appropriate to evaluate the theoretical expressions presented above.

XIII. ATTENUATION AND THE MATERIAL MEMORY INDEX, *n*

An important parameter characterizing a sediment is the positive exponent, n, in the memory function [Eq. (6)]. The smaller the value of n, the longer the memory of the material, and *vice versa*. Now, the frequency-independent component of the wave speed, c_p, in Eq. (64) and the mechanical properties of the sediment are independent of n, and thus the correlations shown in Figs. 8–10 are unaffected by the value of n. Only the magnitude of the attenuation, β_p, as given by Eq. (24b), depends on n, a fact which is important in interpreting the highly variable and complicated nature of the level of attenuation observed in nominally similar marine sediments. Some of the mysteries surrounding attenuation in marine sediments are discussed at length by Hamilton.[18]

Incidentally, in a number of his papers, Hamilton expresses the attenuation coefficient in the form

$$\alpha_H = k_H f^m, \tag{67}$$

where α_H is in dB/m, f is frequency in kHz, m is the exponent of frequency, taken here to be unity, and k_H is a constant for a given material. In reporting levels of attenuation in sediments, it has become fairly common practice to cite values of $k_H$in dB/(m kHz), the implicit assumption being that the attenuation scales as the first power of frequency. By comparing Eqs. (26) and (67), it can be seen that k_H depends on the wave speed, c_p, which is usually reported with the attenuation. The conversion relationship between the dimensionless loss tangent, β_p, in Eq. (26) and k_H is

$$\beta_p = 1.83.10^{-5} c_p k_H. \tag{68}$$

The variability of the attenuation in sediments is illustrated in Fig. 11, which shows measurements of the loss tangent, β_p, as a function of the mean grain size, as reported by Hamilton,[18] Richardson,[53] and Richardson and Briggs.[54] The attenuation data are much more scattered than the wave

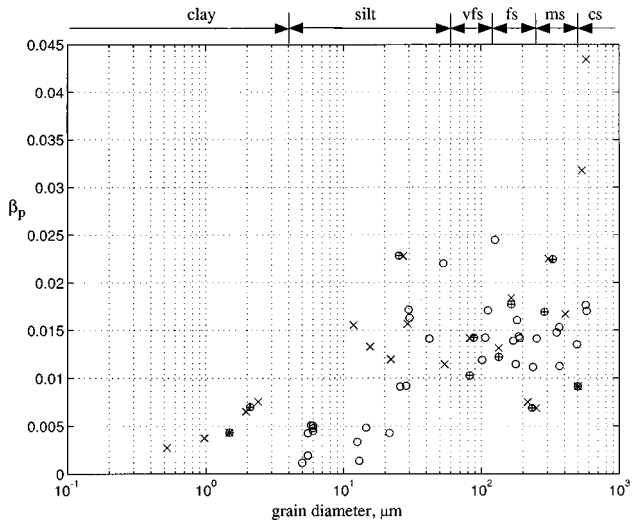

FIG. 11. Plot of loss tangent, β_p, against grain size, u_g. The symbols represent data published by Hamilton (Ref. 18) (○), Richardson (Ref. 53) (⊕), and Richardson and Briggs (Ref. 54) (x). The key to the sediment type is: cs=coarse sand; ms=medium sand; fs=fine sand; vfs=very fine sand.

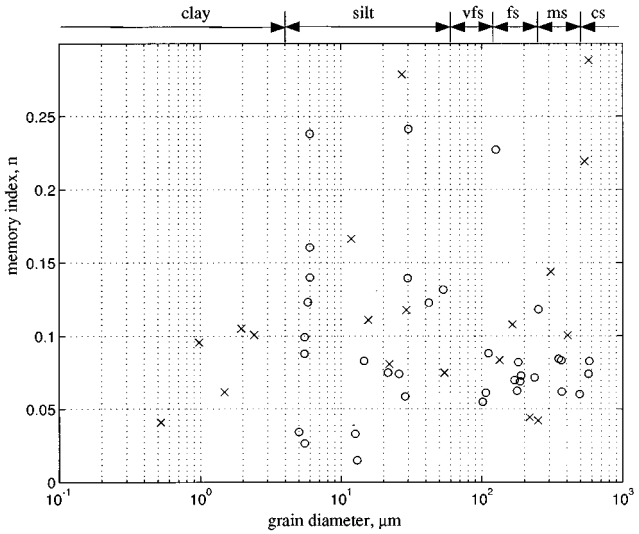

FIG. 13. The memory index n as a function of the grain diameter. The symbols, representing experimental values derived from published data, are as identified in the legend to Fig. 12, and the key to the sediment type is: cs=coarse sand; ms=medium sand; fs=fine sand; vfs=very fine sand.

speed measurements in Figs. 8–10. According to Eq. (24b), the large variability in β_p could originate either with the loss parameter χ_f or with the memory index n. Now, the coefficient χ_f is also important in determining the wave speed [Eq. (25)]; but, as Figs. 8–10 illustrate, the wave speed shows relatively little scatter, following reasonably well-defined trends. This stable behavior suggests that χ_f is itself fairly well-behaved and is not responsible for the variability in β_p. Further support for this conclusion is evident in Fig. 12, which shows χ_f as computed from published measurements of sound speed, porosity, density, and grain size,[18,54] using an inverted form of Eq. (25):

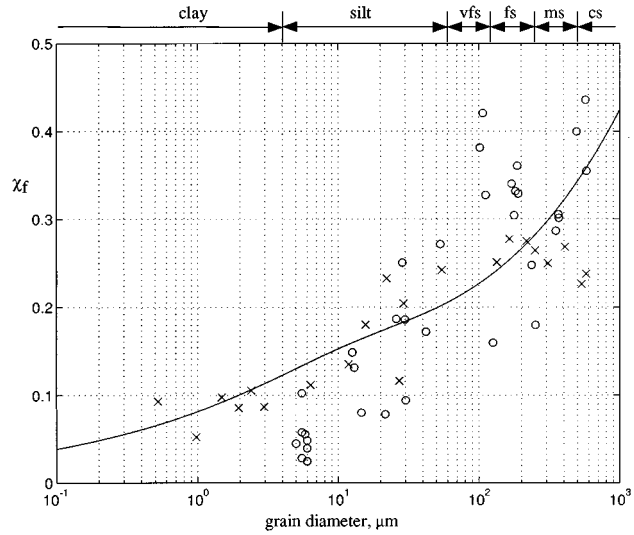

FIG. 12. Plot of the attenuation coefficient, χ_f, versus grain size. The solid line is the theoretical curve from Eq. (62) and the symbols represent experimental values derived from data published by Hamilton (Ref. 18) (○), and Richardson and Briggs (Ref. 54) (x). The key to the sediment type is: cs=coarse sand; ms=medium sand; fs=fine sand; vfs=very fine sand.

$$\chi_f = \frac{c_p^2 - c_0^2}{c_0^2}. \tag{69}$$

To generate the points in the figure from this expression, c_0 was computed from Wood's equation using measured values of density and porosity. The solid line in the figure is the theoretical expression for χ_f in Eq. (62). It can be seen that the values of χ_f derived from data show some scatter about the theoretical curve but not sufficient to account for the observed variability in the attenuation.

If χ_f is not responsible for the scatter in the attenuation data, the culprit must be the memory index n (assuming that the variability is genuine and not an artifact arising from, say, scattering or experimental error). This is confirmed by estimating n from attenuation measurements,[18,54] taken in conjunction with the values of χ_f shown in Fig. 12, using an inverted form of Eq. (24b):

$$n = \frac{4\beta_p}{\pi} \frac{(1+\chi_f)}{\chi_f}. \tag{70}$$

Figure 13 shows the resultant values of n as a function of the grain size. It is evident that n varies wildly, even for sediments with similar grain size. For example, the values of n for the 8 nominally identical fine-slit sediments, with mean grain size around 5–6 μm, range from 0.03 to 0.24, that is, a factor of 8 between the highest and lowest values of n in these otherwise similar materials. (For these particular materials, the reported values of the porosity and bulk density are $N \approx 0.8$ and $\rho_0 \approx 1330$ kg/m^3, respectively.) The mean value of all the points in the Fig. 13 is $\overline{n} = 0.1$, and the standard deviation about the mean is $\sigma_n = 0.06$, which is comparable with the mean, indicative of the high level of scatter.

The widely spread distribution of data points in Fig. 13, following no obvious trend, identifies the principal cause of scatter in the attenuation measurements (Fig. 11) as the exponent, n, of the memory function in Eq. (6). Why should n

show such variability, particularly for macroscopically similar sediments? A plausible reason could be that the length of the memory is very sensitive to the nature of the bonding between mineral grains. This could be affected by the compactness of the sediment, overburden pressure, sharpness of the grains, and perhaps other factors. The actual interparticle forces involved depend on the microstructure and physicochemical nature of the sediment grains, as discussed by Hamilton,[18] but such issues are beyond the scope of the present discussion.

The question of whether the magnitude of the attenuation in marine sediments, β_p, can be predicted, given macroscopic, mechanical information such as particle size or porosity, is important in connection with applications in geophysics and underwater acoustics. On the basis of the spread of the data in Figs. 11 and 13, it would appear that any such prediction could be considerably in error, since there is little correlation between attenuation and, say, particle size. The memory index n, which determines the loss tangent, β_p, is probably governed by microscopic interactions between mineral grains, rather than the macroscopic, mechanical properties of the sediment. These microscopic forces need to be characterized if satisfactory predictions of the level of attenuation are to be achieved.

XIV. CONCLUDING REMARKS

The acoustic properties of marine sediments are of practical interest to underwater acousticians concerned with the prediction of acoustic propagation loss, and to seismologists, geophysicists and geologists in connection with offshore oil and gas exploration. Acoustic attenuation is central to these investigations and accordingly has been the subject of very extensive research. There is now considerable evidence to support the view that in many unconsolidated marine sediments the attenuation scales as the first power of frequency over some six decades of frequency. A satisfactory explanation of this phenomenon has not been readily forthcoming.

In the unified theory of sediment acoustics developed in this article, the medium is treated as a fluid that supports a previously unexplored form of intergranular dissipation. The characteristic feature of the new loss mechanism is hysteresis, that is, the frictional stress at intergrain contacts exhibits a memory. The linear scaling of attenuation with frequency emerges quite naturally from the analysis, and the compressional wave speed is shown to exhibit logarithmic dispersion, although at such a low level as to be negligible in most but not all circumstances. According to the theory, pulse propagation in the medium is strictly causal, as of course it must be, although a simple (but fallacious) Fourier inversion argument, which neglects the tiny level of dispersion, would seem to suggest otherwise. This apparent violation of causality has fueled many a debate in the literature. Without doubt the inter-relationships between attenuation, dispersion, and causality in the context of sediments are subtle but not pathological.

To augment the acoustic theory, a new model of the mechanical properties of sediments is developed, based on the idea of randomly packed, rough mineral grains. When the mechanical model is coupled to the wave theory through a simple relationship between a frictional coefficient and the grain size, expressions are obtained that relate the acoustic properties (wave speed and attenuation) to the mechanical properties (grain size, density, and porosity). As far as the wave speed is concerned, these theoretical correlations show very nice agreement with published data.

The corresponding relationships for the magnitude of the attenuation cannot be easily compared with data, because measurements of attenuation show a high degree of variability for nominally identical sediments. In other words, the level of attenuation does not correlate well with the mechanical properties of the sediment. The new theory has been used to trace the cause of the scatter in the attenuation data back to the material memory function. The level of attenuation appears to be governed by the length of the memory, which could be very sensitive to interparticle bonding forces. Such forces, acting on a microscopic scale, may be very different in otherwise similar materials, due to factors such as compactness, overburden pressure and physico-chemical effects. If this interpretation is correct, it will be difficult to make a prediction of the level of attenuation in a sediment with any degree of confidence until the connection between particle bonding and the material memory function has been established.

In this article, the analysis has concentrated on compressional wave propagation in an unbounded sediment. Shear waves have been neglected in the analysis, even though saturated marine sediments are known to support shear, albeit with wave speeds much slower than those in consolidated rocks. By extending the theoretical arguments developed here in connection with compressional waves, the properties of shear waves in unconsolidated sediments will be established in a second paper on the geoacoustic properties of granular materials. A third paper in the series will address interface wave propagation at the sediment–seawater boundary, on the assumption that the rigidity in the sediment arises solely from inter-granular dissipation.

ACKNOWLEDGMENTS

I have benefited from many discussions with Dr. Grant Deane on attenuation in marine sediments. Dr. Michael Richardson very kindly reviewed the paper in great detail and made many suggestions that lead to a much improved treatment of the mechanical properties of sediments. This research was supported by the Office of Naval Research under Contract No. N00014-91-J-1118, for which I am grateful.

[1] A. C. Kibblewhite, ''Attenuation of sound in marine sediments: A review with emphasis on new low frequency data,'' J. Acoust. Soc. Am. **86**, 716–738 (1989).
[2] R. D. Mindlin, ''Compliance of elastic bodies in contact,'' J. Appl. Mech. **16**, 259–268 (1949).
[3] M. N. Toksöz, D. H. Johnston, and A. Timur, ''Attenuation of seismic waves in dry and saturated rocks, I. Laboratory measurements,'' Geophysics **44**, 681–690 (1979).
[4] D. H. Johnston, M. N. Toksöz, and A. Timur, ''Attenuation of seismic waves in dry and saturated rocks, II. Mechanisms,'' Geophysics **44**, 691–711 (1979).
[5] K. W. Winkler and A. Nur, ''Seismic attenuation: Effects of pore fluids and frictional sliding,'' Geophysics **47**, 1–15 (1982).

[6] E. L. Hamilton, ''Sound attenuation as a function of depth in the sea floor,'' J. Acoust. Soc. Am. **59**, 528–535 (1976).
[7] E. L. Hamilton, ''Acoustic properties of sediments,'' in *Acoustics and the Ocean Bottom*, edited by A. Lara-Saenz, C. Ranz Cuierra, and C. Carbo-Fité (Consejo Superior de Investigacions Investigacions Cientificas, Madrid, 1987), pp. 3–58.
[8] L. Bjørnø, ''Features of the linear and non-linear acoustics of water-saturated marine sediments,'' Technical University of Denmark, Report number AFM 76-06 (1976).
[9] M. N. Toksöz and D. H. Johnston, ''Seismic Wave Attenuation,'' in *Geophysics Reprint Series, No. 2* (Society of Exploration Geophysicists, Tulsa, OK, 1981).
[10] E. Strick, ''Predicted pedestal effect for pulse propagation in constant-*Q* solids,'' Geophysics **35**, 387–403 (1970).
[11] R. W. Morse, ''Acoustic propagation in granular media,'' J. Acoust. Soc. Am. **24**, 696–700 (1952).
[12] J. W. S. Baron Rayleigh, *The Theory of Sound* (Dover, New York, 1945).
[13] J. E. White, *Underground Sound: Application of Seismic Waves* (Elsevier, Amsterdam, 1983).
[14] G. K. Batchelor, *An Introduction to Fluid Dynamics* (Cambridge U.P., Cambridge, 1967).
[15] P. M. Morse and K. U. Ingaard, *Theoretical Acoustics, International Series in Pure and Applied Physics* (McGraw-Hill, New York, 1968).
[16] C. W. Horton, Sr., ''Dispersion relationships in sediments and sea water,'' J. Acoust. Soc. Am. **55**, 547–549 (1974).
[17] F. J. McDonal, F. A. Angona, R. L. Mills, R. L. Sengbush, R. G. Van Nostrand, and J. E. White, ''Attenuation of shear and compressional waves in Pierre shale,'' Geophysics **23**, 421–439 (1958).
[18] E. L. Hamilton, ''Compressional wave attenuation in marine sediments,'' Geophysics **37**, 620–646 (1972).
[19] C. W. Horton, Sr., ''Comment on 'Kramers–Kronig relationship between ultrasonic attenuation and phase velocity' [J. Acoust. Soc. Am. **69**, 696–701 (1981)],'' J. Acoust. Soc. Am. **70**, 1182 (1981).
[20] M. O'Donnell, E. T. Jaynes, and J. G. Miller, ''Kramers–Kronig relationship between ultrasonic attenuation and phase velocity,'' J. Acoust. Soc. Am. **69**, 696–701 (1981).
[21] D. J. Wingham, ''The dispersion of sound in sediment,'' J. Acoust. Soc. Am. **78**, 1757–1760 (1985).
[22] E. L. Hamilton, ''Geoacoustic models of the sea floor,'' in *Physics of Sound in Marine Sediments* (Plenum, New York, 1974), pp. 181–221.
[23] E. L. Hamilton, ''Geoacoustic modeling of the sea floor,'' J. Acoust. Soc. Am. **68**, 1313–1336 (1980).
[24] M. A. Biot, ''Theory of propagation of elastic waves in a fluid-saturated porous solid: I. Low-frequency range,'' J. Acoust. Soc. Am. **28**, 168–178 (1956).
[25] M. A. Biot, ''Theory of propagation of elastic waves in a fluid-saturated porous solid: II. Higher frequency range,'' J. Acoust. Soc. Am. **28**, 179–191 (1956).
[26] M. A. Biot, ''Mechanics of deformation and acoustic propagation in porous media,'' J. Appl. Phys. **33**, 1482–1498 (1962).
[27] R. D. Stoll, *Sediment Acoustics, Lecture Notes on Earth Sciences* (Springer-Verlag, Berlin, 1989).
[28] J. B. Walsh, ''Seismic wave attenuation in rock due to friction,'' J. Geophys. Res. **71**, 2591–2599 (1966).
[29] W. P. Mason, ''Internal friction mechanism that produces an attenuation in the Earth's crust proportional to frequency,'' J. Geophys. Res. **74**, 4963–4966 (1969).
[30] M. D. Verweij, ''Modeling space-time domain acoustic wave fields in media with attenuation: The symbolic manipulation approach,'' J. Acoust. Soc. Am. **97**, 831–843 (1995).
[31] M. D. Verweij, ''Transient acoustic wave modeling: Higher-order Wetnzel–Kramers–Brillouin–Jeffreys asymptotics and symbolic manipulation,'' J. Acoust. Soc. Am. **92**, 2223–2238 (1992).
[32] A. T. de Hoop, ''Acoustic radiation from an impulsive point source in a continuously layered fluid—An analysis based on the Cagniard method,'' J. Acoust. Soc. Am. **88**, 2376–2388 (1990).
[33] A. T. de Hoop, ''Similarity analysis for the elastic wave motion in a dissipative solid under a global relaxation law,'' in *IUTAM Symposium—Nonlinear Waves in Solids*, edited by J. L. Wegener and F. R. Norwood (American Society of Mechanical Engineers, Fairfield, NJ, 1995), p. 77–82.
[34] G. B. Deane, ''Internal friction and boundary conditions in lossy fluid sea beds,'' J. Acoust. Soc. Am. **101**, 233–240 (1997).
[35] J. D. Achenbach, *Wave Propagation in Elastic Solids, Applied Mathematics and Mechanics* (North-Holland, Amsterdam, 1975).
[36] M. A. Biot, ''Generalized theory of acoustic propagation in porous dissipative media,'' J. Acoust. Soc. Am. **34**, 1254–1264 (1962).
[37] M. J. Buckingham, ''Acoustic pulse propagation in dispersive media,'' in *New Perspectives on Problems in Classical and Quantum Physics* (Gordon and Breach, New York, in press).
[38] K. W. Winkler, ''Frequency dependent ultrasonic properties of high-porosity sandstones,'' J. Geophys. Res. **88**, 9493–9499 (1983).
[39] W. T. Born, ''The attenuation constant of earth materials,'' Geophysics **6**, 132–148 (1941).
[40] A. B. Wood, *A Textbook of Sound* (Bell and Sons, London, 1964).
[41] J. C. Molis and N. P. Chotiros, ''A measurement of grain bulk modulus of sands,'' J. Acoust. Soc. Am. **91**, 2463 (A;1992).
[42] N. P. Chotiros, ''Biot model of sound propagation in water-saturated sand,'' J. Acoust. Soc. Am. **97**, 199–214 (1995).
[43] E. L. Hamilton, ''Prediction of deep-sea sediment properties: state-of-the-art,'' in *Deep-Sea Sediments: Physical and Mechanical Properties*, Vol. 2, edited by A. L. Inderbitzen (Plenum, New York, 1974), pp. 1–43.
[44] E. L. Hamilton, ''Elastic properties of marine sediments,'' J. Geophys. Res. **76**, 579–604 (1971).
[45] F. Gassmann, ''Über die elastizität poröser medien,'' Vierteljahrsscher. Naturforsch. Ges. Zürich, **96**, 1–23 (1951).
[46] F. Gassmann, ''Elastic waves through a packing of spheres,'' Geophysics **16**, 673–685 (), and **18**, 269 (1951).
[47] E. L. Hamilton, ''Sound velocity and related properties of marine sediments, North Pacific,'' J. Geophys. Res. **75**, 4423–4446 (1970).
[48] P. C. Gasson, *Geometry of Spatial Forms* (Horwood, Chichester, 1983).
[49] O. K. Rice, ''On the statistical mechanics of liquids, and the gas of hard elastic spheres,'' J. Chem. Phys. **12**, 1–18 (1944).
[50] M. D. Richardson and K. B. Briggs, ''*In situ* and laboratory geoacoustic measurements in soft mud and hard-packed sand sediments: Implications for high-frequency acoustic propagation and scattering,'' Geo-Marine Lett. **16**, 196–203 (1996).
[51] M. D. Richardson, personal communication (1997).
[52] S. Timoshenko and J. N. Goodier, *Theory of Elasticity* (McGraw-Hill, New York, 1951).
[53] M. D. Richardson, ''Spatial variability of surficial shallow water sediment,'' in *Ocean-Seismo Acoustics*, edited by T. Akal and J. M. Berkson (Plenum, New York, 1986), pp. 527–536.
[54] M. D. Richardson and K. B. Briggs, ''On the use of acoustic impedance values to determine sediment properties,'' in Proc. Inst. Acoust. **15**, Pt. 2, 15–24 (1993).